Acta Biomaterialia 118 (2020) 44–53

Contents lists available at ScienceDirect

Acta Biomaterialia

journal homepage: www.elsevier.com/locate/actbio

Construction of a simple and intelligent DNA-based computing system for multiplexing logic operations

Hongmei Geng[a,b], Ze Yin[f], Chunyang Zhou[a,c,d,*], Chunlei Guo[e,*]

[a] The Photonics Laboratory, State Key Laboratory of Applied Optics, Changchun Institute of Optics, Fine Mechanics and Physics, Chinese Academy of Sciences, Changchun, Jilin, 130033, China
[b] University of Chinese Academy of Sciences, Beijing 100049, China
[c] Institute of Molecular Medicine, State Key Laboratory of Oncogenes and Related Genes, Renji Hospital, School of Medicine, Shanghai Jiao Tong University, Shanghai 200127, China
[d] Department of Biomedical Engineering, Emory University, Atlanta, Georgia 30322, United States
[e] The Institute of Optics, University of Rochester, Rochester, New York, 14627, United States
[f] Department of Biomedical Engineering, Texas A&M University, College Station, Texas 77843, United States

ARTICLE INFO

Article history:
Received 8 May 2020
Revised 25 September 2020
Accepted 29 September 2020
Available online 6 October 2020

Keywords:
Square root
Cube root
Mathematic calculations
DNA hybridization

ABSTRACT

Over the past few decades, DNA-based computing technology has become a rapidly developing technology and shown remarkable capabilities in handling complex computational problems. However, most of the logical operations that DNA computer can achieve are still very basic or using large-scale operations to realize complex functions, especially in mathematics. Graphene oxide (GO) is an ideal nanomaterial for biological computing, which has been used in our previous work to perform basic logic operations. Here, we utilize GO to implement far more complex and large-scale logical computing. For the first time, in this work, we utilize the unique interaction between GO and a variety of classified single-stranded DNAs as the reaction platform, by segmenting and encoding the DNA sequences, and programming the interactions between inputs and between the inputs and reaction platform, two relative large-scale logic operations, 6-bit square-root and 9-bit cube-root logical circuits are realized. This study provides a simple but efficient method for advanced and large-scale logical mathematic operations in biotechnology, opening a new horizon for building biocomputer-based innovative functional devices.

Statement of significance

The overarching objective of this paper is to construct a novel DNA mathematic calculating system driven by the displacement of DNA strands and graphene oxide (GO). Based on the same DNA/GO platform and DNA hybridization mechanism, two relative large-scale mathematic calculations, 6-bit square-root and 9-bit cube-root logical operations are both realized simultaneously through the reactions between the inputs and between the inputs and the platform. This work provides an easy approach for DNA computing technology to implement novel functional devices and concrete large-scale mathematic calculations. This study is expected to realize large-scale and more complex mathematic calculations and avoid the problems of design complexity and manufacturing cost compared to the logical circuits in traditional computing.

1. Introduction

Today, silicon-based computer plays a dominant role in technological fields [1–2]. Modern computing is based on the Boolean logic operations, binary numbers are used to perform logical operations that assigned “true” to “1” in bit form and “false” to “0” [3]. While facing the challenges of the miniaturization/limited capacity of silicon and the ever-increasing computational demands, other biomolecules are examined as an alternative to silicon for logical operations, which is expected to solve complex problems that are difficult to handle by traditional silicon-based computers [4–12]. A number of bottom-up approaches have led to some successful examples, such as Turing machine simulations [13], chemical reaction networks [14–17], automated cellar simulations [13], and molecular logical computation [18–21]. Different from silicon-based logic computing, molecular logical computation utilizes binary-encoded biomolecules as inputs (absence as “0”/presence as “1”) and optical/electrochemical signals as outputs (low as “0”/high as “1”). Among various biomolecule-based logic systems, DNA is an outstanding candidate because of its high computing capability, cost-

* Corresponding authors.
E-mail address: cyzhou@ciomp.ac.cn (C. Zhou).

https://doi.org/10.1016/j.actbio.2020.09.054
1742-7061/

effectiveness, flexible design, and controllable structure. Particularly, DNA pairing is governed by the Watson-Crick base pairing, i.e., A binds to T and C binds to G [22–27].

In recent years, many DNA logical circuits are constructed to implement multiple functions based on enzyme-catalyzed reactions [28,29], functional DNA structures [30,31] and DNA-based hybridizations [32–36]. Many basic/advanced logical DNA operations, such as AND, OR, XOR, INHIBIT, XNOR, NAND, NOR, IMPLICATION logical gates or even functional logic circuits, are realized through rigorous design [37–40]. However, despite significant advancements in DNA computing, there are still a range of restrictions. First of all, most DNA logic devices currently can only produce monochromic or undetectable optical signals, which largely restrict the further development of biocomputing complexity for more outputs. Secondly, most of the DNA logic circuits are still incapable of realizing complex mathematical operations, such as the square root logic operation and the cube root calculating operation, which could only be carried out to realize square root circuits [26,50]. Thirdly, the lack of an integration platform to integrate multiplex logic operations into one platform is also a challenge. In this work, an intelligent universal system is constructed to realize not only relative large-scale mathematical calculations of square root logic operations but also cube root logic operations. Furthermore, the logic devices with multiple outputs developed in this work can be easily integrated into higher-order logic arrays or even networks through multiple parallel operations, similar to wireless integration in electronics [26,41].

As a kind of water-soluble material, graphene oxide (GO) has excellent catalytic, electronic, and optical properties, and has attracted a great amount of attention due to its physical and chemical characters. Particularly, GO has the property of quenching the fluorescence nearby through the fluorescence resonant energy transfer (FRET) [42,43]. Interestingly, GOs presents the ability of adsorbing single-stranded DNA on its surface due to the high affinity between them through pi-stacking interactions. However, GO shows a weak affinity to duplex DNA, which allows for flexible regulation of the output signals during biomolecular logic operations [44–51]. Based on the above properties of GO, in this work, for the first time, two logical operations, 6-bit square-root and 9-bit cube-root logical circuits, are designed based on the unique GO/DNA platform to implement the relative large-scale biomolecular-based mathematical calculations by segmenting and encoding the DNA sequences, and programming the interactions between inputs and between the inputs and reaction platform, the 6-bit square-root and 9-bit cube-root mathematic calculations are successfully realized. More complex and systematic logic operations can be realized in future studies to achieve further integration and modularization of biological computing.

2. Experimental section

2.1. Materials and apparatus

All the DNA strands used in this work are purchased from Sangon Biotechnology Company (Shanghai, China) and the DNA sequences are listed in the Supporting Information (Table S1). The Acrylamide, ammonium persulfate, Tris (hydroxymethyl) aminomethane and Boric acid are purchased from Aladdin biochemical technology co. LTD.. EDTA is purchased from Sangon Biotechnology Company. All chemicals used in this work are of analytical reagent without further purification. The concentrations of all the DNA sequences are quantified by Nanodrop One from Thermo with the following extinction coefficients (ε260 nm, $M^{-1}cm^{-1}$): A = 15,400, T = 8700, G = 11,500, C = 7400. All solutions have been prepared by ultrapure water (18.2 MΩ•cm) obtained from Milli-Q purification system.

The fluorescence emission spectra are obtained from the Cary Eclipse Fluorescence Spectrophotometer purchased from Agilent Technologies in Tris–HCl buffer (20 mM Tris–HCl, 200 mM KCl, 10 mM $MgCl_2$, pH 8.0) in room temperature. The excitation of ROX, HEX and Cy5 are performed at 585, 537 and 632 nm, respectively. The emission wavelengths of the ROX, HEX and Cy5 are recorded at 605, 556 and 663 nm. The native polyacrylamide gel electrophoresis experiments are done in the electrophoresis tank purchased from Bio Rad. The gel images are obtained by the BioDoc-It2 Imager from UVP.

2.2. Preparation of GO

Graphene oxide is synthesized based on Hummers work [54]. In brief, graphite powder (5 g), P_2O_5 (5 g) and $K_2S_2O_8$ (5 g) are mixed and added to H_2SO_4 solution (98%, 35 mL). Then, the mixture is heated to 80 °C for 4 h under constant stirring and cooled down. After adding water, the product is collected and centrifuged and then filtered to remove the acid. Next, the precipitate is dissolved in H_2SO_4 and $KMnO_4$ (30 g) is added under constant stir. After 24 h, H_2O (1200 mL) is added and stirred for 3 h. Finally, after adding H_2O_2 (35%, 40 mL) to the solution, the color of the mixture is changed to yellow. The product is filtered and washed using HCl and H_2O, and then loaded in dialysis tubes and purified for 2 weeks to remove any remaining metal.

2.3. Statistical analysis

Before the operation of DNA-based square root and cube root logic circuits, the optimized experiments have been done by the hybridization of DNA strands. First of all, the optimized concentration of the GO in the platform is confirmed based on the fluorescence intensity of ROX, HEX and Cy5 that modified on the fixed concentrations of F1, F2 and F3 (100 nM) (in Fig. S2). Secondly, the concentrations of the individual-DNA strands on the surface of GO are optimized to perform at a lower background. The concentrations of the F1, F2, and F3 are confirmed to be 100 nM, 100 nM and 100 nM, respectively. Thirdly, for the square-root DNA logic operation, the optimized concentrations of the inputs (S1, S2, S3, S4, S5 and S6) are confirmed based on the fluorescence intensity of ROX, HEX, and Cy5 to be 550 nM, 500 nM, 550 nM, 550 nM, 1100 nM, and 800 nM, respectively (Fig. S3). Then, the optimized concentrations of the inputs (C6, C7, C8 and C9) in the logic circuit of cube root are confirmed based on the fluorescence intensity of ROX, HEX, and Cy5 as 1400 nM, 1200 nM, 1100 nM, and 1000 nM, respectively (Fig. S6). Particularly, the input strands of DNA (C1, C2, C3 and C4) in the cube root operation have the same sequences and the same reactions as the inputs (S1, S2, S3 and S4) in the square root system. Therefore, the optimized concentrations of the inputs (C1, C2, C3 and C4) in the logic circuit of cube root are confirmed as 550 nM, 500 nM, 550 nM, and 550 nM, which are based on the fluorescence intensity of ROX, HEX, and Cy5.

2.4. Logic circuit operation

The DNA sequences are dissolved in deionized water as stock solution and diluted with Tris–HCl buffer (20 mM Tris–HCl, 10 mM $MgCl_2$, 200 mM KCl, pH 8.0) for the hybridization in the logic operations. Before used, the diluted DNA solutions are heated at 90 °C for 10 min and then gradually cooled down to the room temperature. The platform of the square-root and cube-root system is prepared by mixing GO (2.5 μg/mL) and DNAs with fluorephore (100 nM, F1, F2 and F3) for 10 min at room temperature. After that, calculations can be activated by adding corresponding inputs according to the truth table for the realization of square-root and cube-root logic computing. The optimized concentrations of inputs

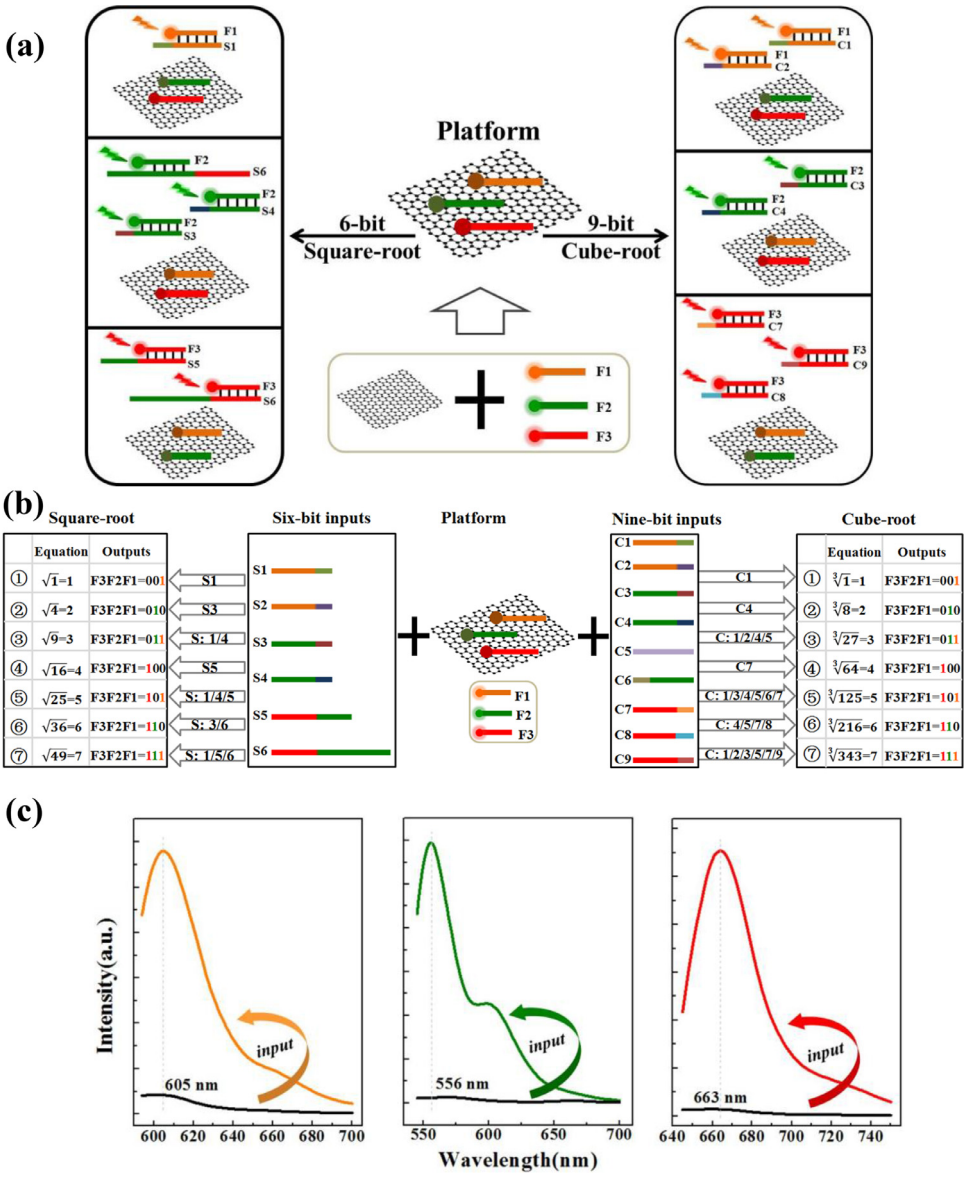

Fig. 1. The summary of the hybridization reaction mechanism for the square-root and cube-root operation. (a) The hybridization mechanism of the square-root and cube-root operations. Left side: the hybridization mechanism of square-root operation between inputs and the DNA/GO platform. Right side: the hybridization mechanism of cube-root operation between inputs and the DNA/GO platform. (b) The interactions between the inputs and the DNA/GO platform for 6-bit the square-root and the 9-bit cube-root mathematic calculations. (c) The fluorescence changes before and after the inputs are added.

and GO/DNA platform are mixed to a final volume of 400 μL and incubated at room temperature for 30 min. Fluorescence kinetic experiments have been implemented based on DNA/GO platform in our previous work and the reacting time is about 30 min [55].

2.5. Native polyacrylamide gel electrophoresis (PAGE)

Before used, all the DNA stock solutions are diluted to 2 μM with Tris–HCl buffer (20 mM Tris–HCl, 200 mM KCl, 10 mM $MgCl_2$, pH 8.0) and denatured by heating at 90 °C for 10 min. After cooled down to the room temperature slowly, the desired volume of the platform and corresponding inputs are mixed and incubated for 30 min. After the preparation of 15% native polyacrylamide gel, the electrophoresis is conducted in 1×TBE (17.8 mM boric acid, 17.8 mM Tris, 2 mM EDTA, pH 8.0) at a constant voltage of 120 V for about 1 h. Finally, the finished gels are scanned by UV transilluminator.

3. Results and discussions

In this work, in order to develop a programmable method to realize the relative large-scale 6-bit square-root and 9-bit cube root logic circuits, the key mechanism that enables DNA logic circuits to be rationally programmed is based on the powerful DNA hybridization, toehold-mediate DNA strand displacement (TDSD) and interactions between DNA and nanomaterials. The detailed reacting mechanism between single/double DNA and GO is illustrated in Fig. S1. In particular, the interactions of DNAs and GO used in this work can dynamically and flexibly operate the fluorescence-based output signals according to the unique characters of GO, which opens up the possibility of programming DNA/GO platform for larger scale biocomputing. In contrast to previous works, most of them are based on the DNA hybridization, catalytic nucleic acid and enzymes to operate the logical circuits, which largely limit the complexity and reaction environment of the biocomputing. For example, by integrating the basic logic units, Qian and coworkers re-

(a)

Square roots of integers	Inputs						Outputs		
	2^5	2^4	2^3	2^2	2^1	2^0	F3	F2	F1
	S6	S5	S4	S3	S2	S1	(Cy5)	(HEX)	(ROX)
1^2	0	0	0	0	0	1	0	0	1
2^2	0	0	0	1	0	0	0	1	0
3^2	0	0	1	0	0	1	0	1	1
4^2	0	1	0	0	0	0	1	0	0
5^2	0	1	1	0	0	1	1	0	1
6^2	1	0	0	1	0	0	1	1	0
7^2	1	1	0	0	0	1	1	1	1

(b)

Cube roots of integers	Inputs									Outputs		
	2^8	2^7	2^6	2^5	2^4	2^3	2^2	2^1	2^0	F3	F2	F1
	C9	C8	C7	C6	C5	C4	C3	C2	C1	(Cy5)	(HEX)	(ROX)
1^3	0	0	0	0	0	0	0	0	1	0	0	1
2^3	0	0	0	0	0	1	0	0	0	0	1	0
3^3	0	0	0	0	1	1	0	1	1	0	1	1
4^3	0	0	1	0	0	0	0	0	0	1	0	0
5^3	0	0	1	1	1	1	1	0	1	1	0	1
6^3	0	1	1	0	1	1	0	0	0	1	1	0
7^3	1	0	1	0	1	0	1	1	1	1	1	1

Fig. 2. (a) Truth table of the 6-bit square-root logic calculations. (b) Truth table of the 9-bit cube-root logical calculations.

alized the calculation of 4-bit square root logic operation [26]. In our previous work, by utilizing the DNA hybridization and TDST, a 10-bit square-root logic circuit was realized [52]. However, in this work, by programming the hybridization between the input DNAs and DNA/GO reaction platform, two algorithms logic circuits (6-bit square root and 9-bit cube root logic circuits) are realized using the same GO/DNA platform, which shorten the reacting time and complexity compared to strand displacement reaction in our previous work [53].

As shown in Fig. 1a, a multifunctional and high-capacity reacting platform is established, which can calculate the square root of a 6-bit binary number (within the decimal integer 50) or the cube root of 9-bit binary number (within the decimal integer 500). The reacting platform is consisting of GO and a variety of fluorescence modified single-stranded DNAs that adsorb on the surface of GO. In the initial state, three kinds of fluorescent (ROX, HEX and Cy5, emission max at 605 nm, 556 nm and 663 nm) labeled DNAs (F1, F2 and F3) are attached on GO and quenched by it, emitting three low fluorescence signals (Fig. 1c, black curves). In order to realize the 6-bit square root and 9-bit cube root logic operations (truth tables in Fig. 2), there are two aspects to be programmed between the inputs and the platform. First, programming the hybridization reactions between a single input DNA and the platform, which aims to not only realize a part of the relatively simple calculations, but also lay a foundation for the relatively complex calculations. As shown in Fig. 1a, in 6-bit square root logic system, different individual input DNAs can hybridize with its unique fluorescence modified DNA on GO, which can be enhanced to show a high fluorescence output signal (Fig. 1c, the colorful curves). For example, as shown in Fig. 1b, in order to realize the 6-bit square root logic operation (within the decimal integer 50), the ROX fluorescence that modified on F1 is programmed to be lit up by input S1, with the calculating result is decimal integer "$\sqrt{1} = 1$" (F3F2F1 = 001). The HEX fluorescence that modified on F2 is encoded to be lit up by input S3 or S4. Especially, in the case of adding input S3 to the platform, which can calculate the square root decimal integer "4" to be "$\sqrt{4} = 2$" (F3F2F1 = 010). The fluorescence of Cy5 that modified on F3 is encoded to be lightened up by input S5, with the calculation result is decimal integer "$\sqrt{16} = 4$" (F3F2F1 = 100). The input S6 is programmed to hybridize with both F2 and F3, lighting up the fluorescence of HEX and Cy5. Second, programming the hybridization reactions between inputs and between inputs and platform for the realization of other more complex calculations, in which there are multiple input DNAs involved. For example, as shown in Fig. 1b, in the case of calculating the square root of decimal integer "49" in 6-bit square root logic operation, three inputs (S1, S5 and S6) are encoded to add to the platform. At this point, hybridizations occur not only between the inputs, but also between the inputs and the platform. By utilizing the same platform, a 9-bit cube-root logic operation (within the decimal integer 500) can also be realized by

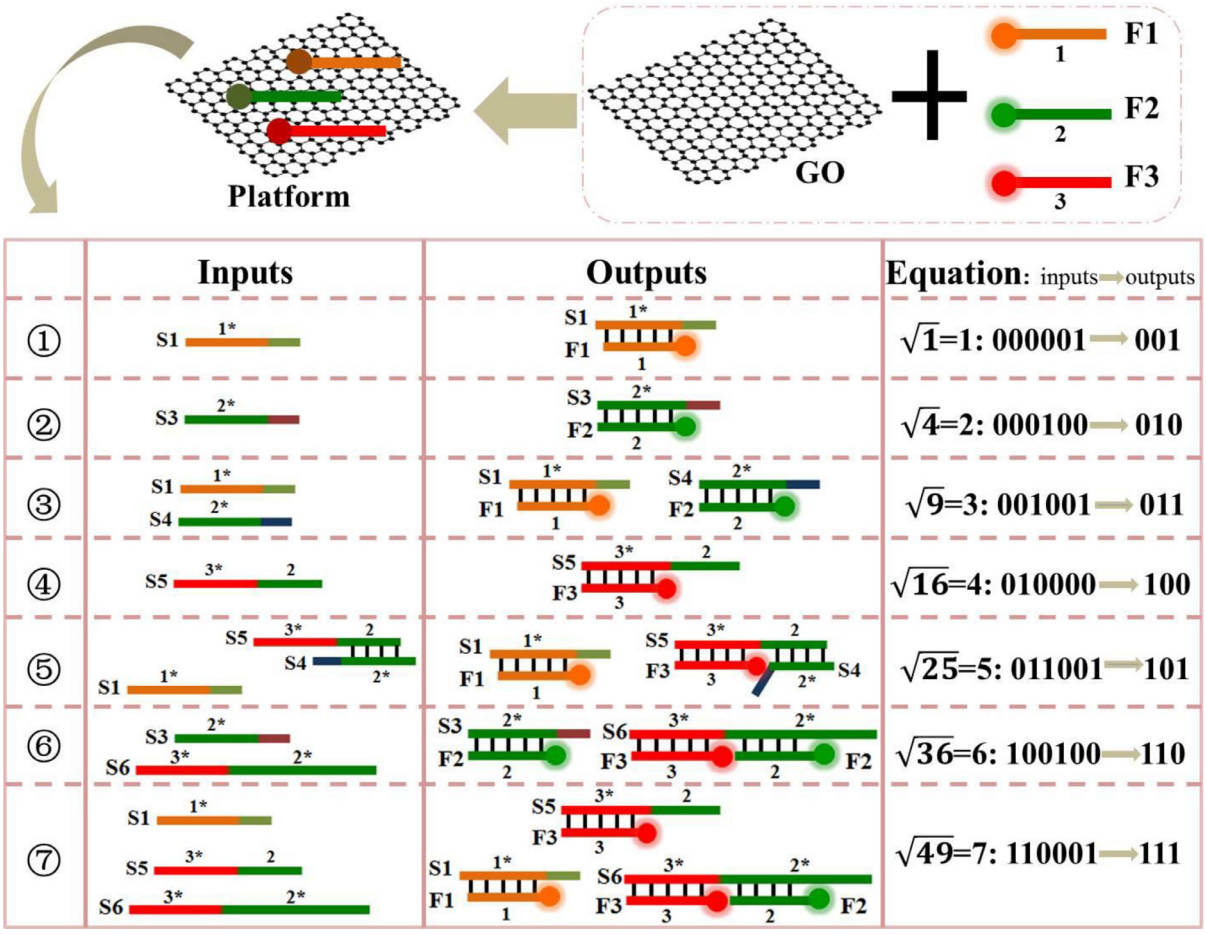

Fig. 3. Reaction mechanism of the 6-bit square root logic operation. The detail hybridization reactions are listed between the six inputs and the DNA/GO platform for the realization of the 6-bit square root mathematic calculation.

encoding the nine inputs (C1-C9) to hybridize with the DNA/GO platform according to the truth table and output the corresponding fluorescence signals (shown in Fig. 1b, 1c).

As shown in Fig. 2a and 2b, in order to calculate the 6-bit square-root and 9-bit cube-root logic operations, the programming values of input variables and corresponding output values are listed, which is the so-called truth table. The truth table can pre-plan and code the logical relationship between the inputs and outputs of logical operations in a binary language. Once the value of the input has been determined, the corresponding output value can be found in the table. For input, the absence of the input is defined as "0", otherwise, it is defined as "1" for presence. For output, the enhanced fluorescence intensity is defined as "1", otherwise, it is defined as "0" for the low fluorescence intensity.

3.1. Square root operation

Fig. 3 shows the working principle for the implementation of the 6-bit square-root logic operation by summarizing the hybridization reactions between inputs and the interactions between inputs and DNA/GO platform. Firstly, the DNA/GO platform is prepared in advance before operating the 6-bit square root logic circuit. The optimized interactions of fluorescence modified DNA (F1, F2 and F3) and GO are studied (Supporting information, Fig. S2 a-c). Different concentrations of the inputs (S1, S2, S3, S4, S5 and S6) are optimized (Fig. S3). As shown in Fig. 3, in the initial state, no input is added, and the three fluorescence signals that are quenched by GO remain low (which is defined as "000" in truth table, with the corresponding fluorescence spectrum in Fig. 4, curve a0, b0 and c0). In the calculation of the square-root decimal integer "1" (binary number of "000,001"), the input S1 (1*) is added to the DNA/GO platform (Fig. 3) and hybridizes with F1 (1), forming the duplex S1/F1 and desorbing from the surface of GO. Such reaction leads to an increased fluorescence of ROX and the relative low fluorescence of HEX and Cy5 (Fig. 4, curve a1, b1, and c1). In this case, the enhanced ROX fluorescence is defined as "1" and the relative low fluorescence of HEX and Cy5 are defined as "0" in truth table (Fig. 2a), representing the square-root calculating result is " $\sqrt{1}=1$" (output binary number of "001"). For the calculation of the decimal integer "2" (binary number of "000,100"), the input S3 (2*) is introduced into the platform and binds with F2 (2) to form the duplex S3/F2 and desorb from the surface of GO. In this case, the HEX fluorescence is increased and defined as "1" (Fig. 4, curve b2). The fluorescence of ROX and Cy5 remain low and are defined as "0" (Fig. 4, curve a2 and c2), illustrating the square-root calculating result is "$\sqrt{4}=2$" (output binary number of "010"). In the calculation of square-root decimal integer "3" (binary number of "001,001"), the inputs S1 (1*) and S4 (2*) are added into the platform and hybridize with F1 and F2 respectively, forming the duplex of S1/F1 and S4/F2 to depart away from GO (Fig. 3). In this case, the fluorescent signals of ROX and HEX are lit up (Fig. 4, curve a3 and b3) and defined as "1", on the contrary, the fluorescent signal of Cy5 remains low (Fig. 4a, curve c3) and is defined as "0", showing the square-root calculation result of "$\sqrt{9}=3$" (output binary number of "011"). In order to implement the square-

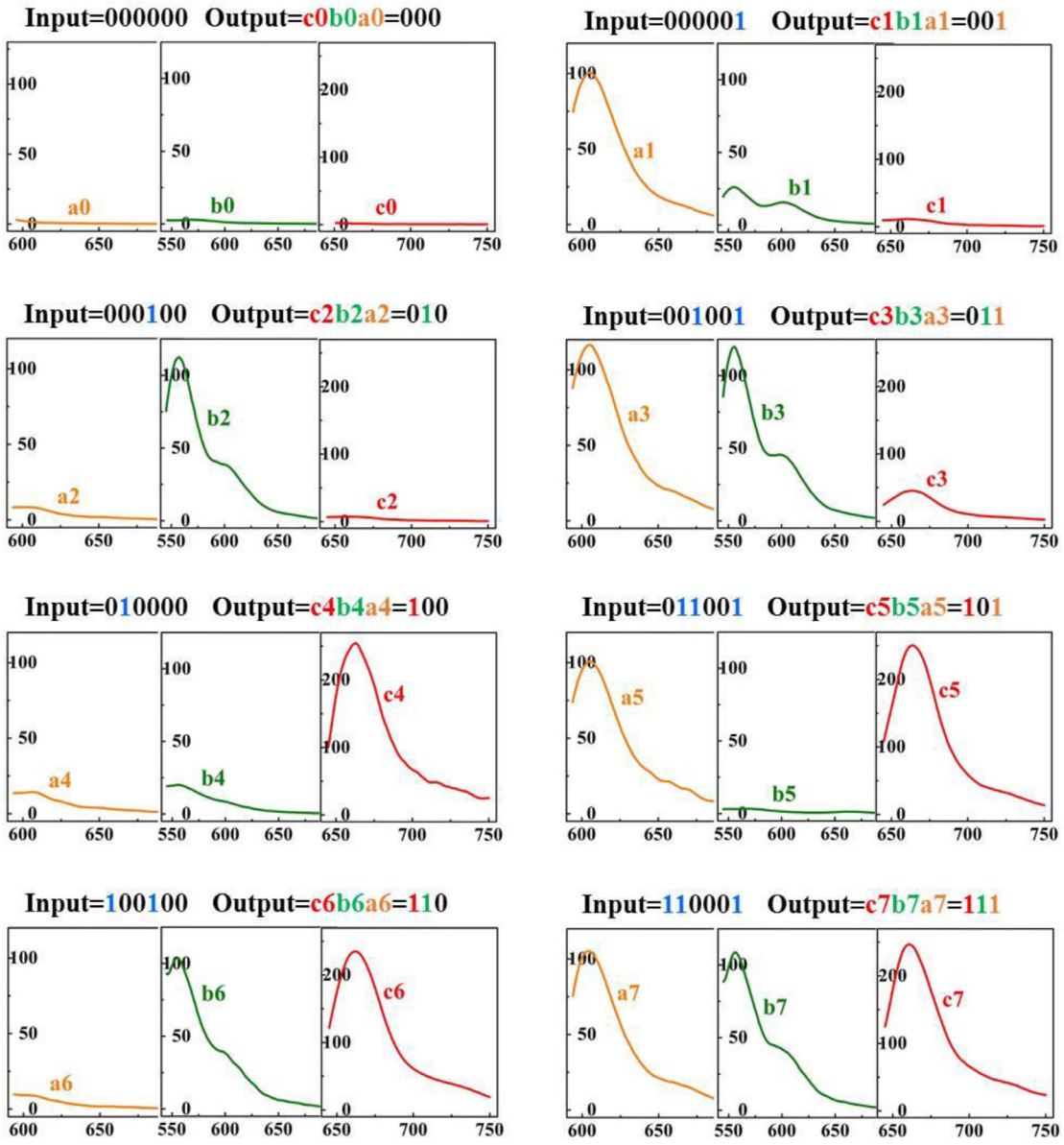

Fig. 4. The fluorescence signal outputs of the platform with the corresponding inputs to demonstrate the successful operation of 6-bit square root mathematic calculations, which is corresponding to Fig. 3.

root decimal integer "4" (binary number of "010,000"), the input S5 (3*−2) is added into the DNA/GO platform and hybridizes with F3 (3*), forming the duplex S5/F3 and desorbing from the surface of GO (Fig. 3). Such hybridization results in an enhanced fluorescence of Cy5 (Fig. 4, curve c4) and relative low signals of ROX and HEX (Fig. 4, curve a4 and b4), representing the calculating result is "$\sqrt{16}=4$" (output binary number of "100"). In order to calculate the square-root decimal integer "5" (binary number of "011,001"), the inputs S1 (1*), S4 (2*) and S5 (3*−2) are encoded to add to the platform. In this case, the input S1 can hybridize with F1. The inputs S4 and S5 have the priority to hybridize with each other and form the duplex S4/S5, which can then hybridize with F3 and form the DNA strand of S4/S5/F3 to desorb from GO. Such reactions light up the fluorescence signals of ROX and Cy5 (Fig. 4, curve a5 and c5), with the HEX fluorescence keeps low-state (Fig. 4, curve b5), representing the square-root calculating result of "$\sqrt{25}=5$" (output binary number of "101"). In the calculation of decimal integer "6" (binary number of "100,100"), inputs S3 (2*) and S6 (2*−3*) are added to the platform. In this case, S3 can hybridize with F2 to form S3/F2. The S6 can hybridize with both F2 and F3 to desorb from GO. Therefore, the fluorescence signals of HEX and Cy5 are enhanced and defined as "1" (Fig. 4, curve b6 and c6), the ROX fluorescence keeps low and is defined as "0" (Fig. 4, curve a6) in truth table, with the square-root calculation result of " $\sqrt{36}=6$" (output binary number of "110"). In order to calculate the square-root decimal integer "7" (binary number of "110,001"), the inputs of S1 (1*), S5 (3*−2) and S6 (2*−3*) are added to GO/DNA platform and hybridize with F1, F2 and F3 respectively, forming the duplex of S1/F1 and S5/F3 and desorbing from GO surface. S6 hybridizes with both F2 and F3 to trigger the signals of HEX and Cy5. In this case, all the fluorescence outputs (ROX, HEX and Cy5) are lit up (Fig. 4, a7, b7 and c7) and defined as "1", with the square-root result of "$\sqrt{49}=7$" (output binary number of "111"). In order to further verify the DNA hybridization between the inputs and the DNA/GO platform in the 6-bit square-root logic system, the native polyacrylamide gel electrophoresis (PAGE) experiments are implemented, with the details explained in Supporting Information (Fig. S4).

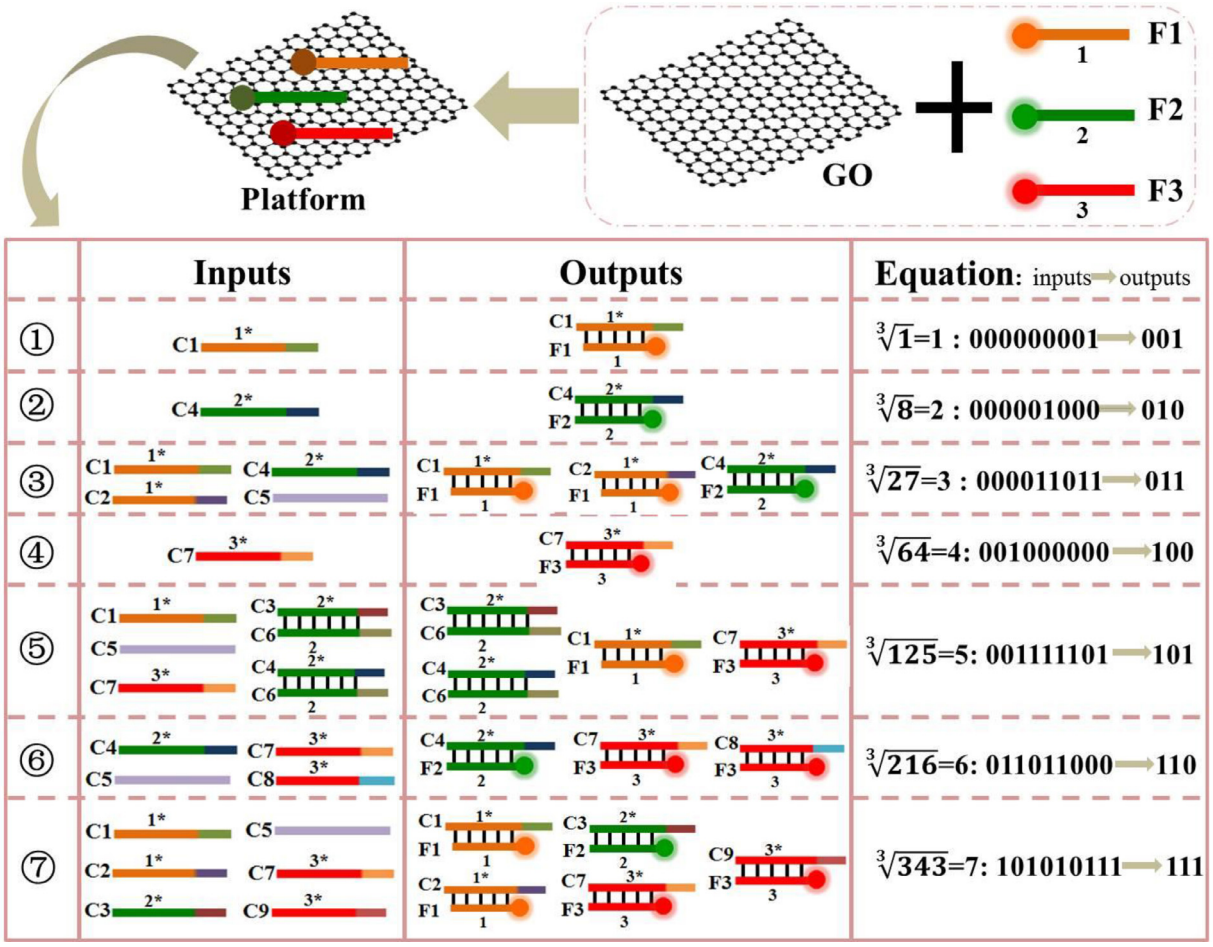

Fig. 5. The detail reaction mechanism of the 9-bit cube root logic operation. The hybridization reactions between the DNA/GO platform and nine inputs for the realization of the 9-bit cube root logic operation.

In order to avoid the influence of experimental errors on the arithmetical operation, a threshold analysis is conducted on the intensity of fluorescence signal, that is, only when the fluorescence intensity is high enough can it be defined as binary "1", otherwise it can be defined as "0". As shown in Fig. S5, the normalized fluorescence intensities of the outputs (ROX, HEX and Cy5) at maximum peaks are plotted to define the threshold value. The function of the threshold value is to make the output signals eliminate interference and still achieve ideal digital ON and OFF levels, despite the possible signal interference in the case of multiple input signals. Also, when some fluorescence background signal inevitably rises caused by experimental errors, it will not exceed the defined threshold value, and it will not affect the operation results.

3.2. Cube root operation

Based on the same multifunctional GO/DNA platform, a 9-bit cube-root logic operation is implemented. Fig. 5 exhibits the working mechanism to implement the 9-bit cube-root logical system by summarizing the interactions between the inputs and DNA/GO platform. Before operating the 9-bit cube-root logical circuits, different concentrations of the inputs (C1, C2, C3, C4, C5, C6, C7, C8 and C9) are optimized (Fig. S3 a-d and Fig. S6 a-d). In the initial state, no input is added, the fluorescence that modified on F1, F2 and F3 are quenched by GO and remain low, which is defined as "000" in truth table (corresponding fluorescence spectrum in Fig. 6, curve a0, b0 and c0). In the cube-root decimal integer "1" (binary number of "000,000,001"), the input C1 is added into the platform and hybridizes with F1 (1) (Fig. 5), enhancing ROX fluorescence to be defined as "1", while the other two fluorescence of HEX and Cy5 remain low (Fig. 6, curve a1, b1 and c1) and are defined as "0" in truth table (Fig. 2b). Such operation represents the cube-root calculation result of "$\sqrt[3]{1} = 1$" (output binary number of "001"). In order to calculate the cube-root decimal integer "2" (binary number of "000,001,000"), the DNA strand C4 (2*) is added into platform and hybridizes with F2 to form the double strands of C4/F2 to desorb from the surface of GO (Fig. 5). In this case, the HEX fluorescence is lit up (Fig. 6, curve b2) and defined as "1", the fluorescence signals of ROX and Cy5 remain relatively low (Fig. 6, curve a2 and c2) and are defined as "0" in truth table, with the calculating result of "$\sqrt[3]{8} = 2$" (output binary number of "010"). In the calculation of cube root decimal integer "3" (the input binary number of "000,011,011"), the inputs of C1 (1*), C2 (1*), C4 (2*) and C5 are introduced into DNA/GO platform. The C1 and C2 are encoded to hybridize with F1 and C4 is encoded to hybridize with F2, forming the duplex strands of C1/F1, C2/F1 and C4/F2 and desorbing from the surface of GO (Fig. 5). In this case, the resulting signals of ROX and HEX are enhanced (Fig. 6, curve a3 and b3) and defined as "1", however, the Cy5 fluorescence remains low (Fig. 6, curve c3) and is defined as "0", with the output signal of "011" and representing the cube-root operation result of "$\sqrt[3]{27} = 3$". In the calculation of cube-root decimal integer "4" (binary input of "001,000,000"), the input C7 is added to the platform and hybridizes with F3, enhancing the fluorescence of ROX that modified on F3 (Fig. 6, curve c4), with the output signal of "100" and representing the calculation

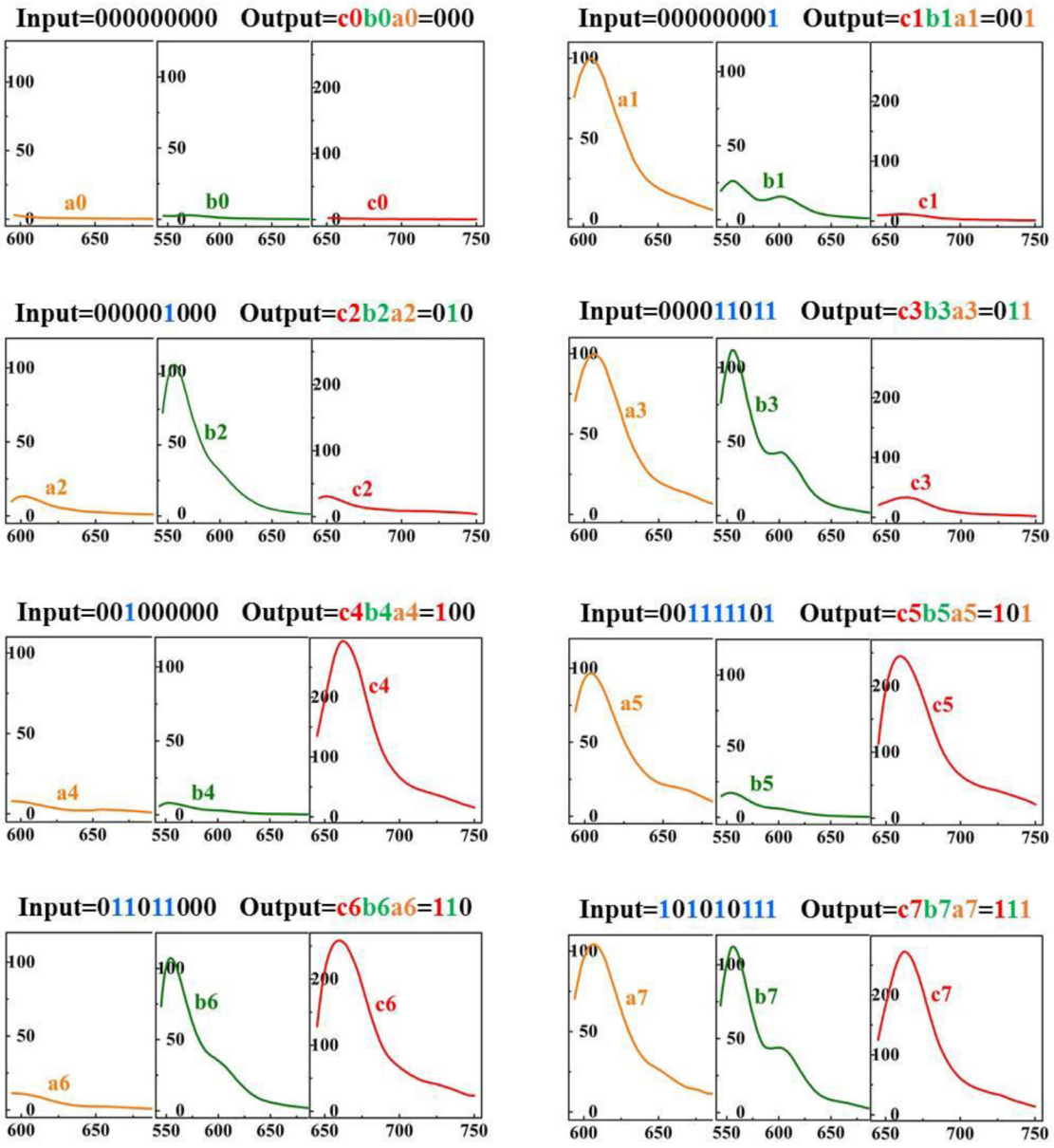

Fig. 6. The fluorescence signal outputs of the platform with the corresponding inputs to demonstrate the successful operation of 9-bit cube root mathematic calculations, which is corresponding to Fig. 5.

result of "$\sqrt[3]{64} = 4$". In order to implement the cube root calculation decimal integer "5" (the input binary number of "001,111,101"), multiple inputs of C1 (1*), C3 (2*), C4 (2*), C5, C6 (2) and C7 (3*) are added to the platform. In this case, the C6 first hybridizes with C3 and C4, forming the duplex of C3/C6 and C4/C6. C1 and C7 hybridize with F1 and F3 respectively to form the duplex of C1/F1 and C7/F3. Therefore, the fluorescence ROX and Cy5 are enhanced to be defined as "1" and the HEX fluorescence remains low to be defined as "0" (Fig. 6, curve a5, b5 and c5), exhibiting the fluorescence output of "101" and corresponding to the 9-bit cube-root mathematic calculation of "$\sqrt[3]{125} = 5$". In calculating the cube-root decimal integer "6" (the binary inputs of "011,011,000"), the inputs C4 (2*), C5, C7 (3*) and C8 (3*) are added to the DNA/GO platform. Both C7 and C8 are encoded to hybridize with F3, forming the duplex of C7/F3 and C8/F3 and desorbing from DNA/GO platform. Also, input C4 is encoded to hybridize with F2 to form the duplex of C4/F2. Therefore, the fluorescence of HEX and Cy5 (Fig. 6, curve b6 and c6) are increased and defined as "1", showing the output fluorescence signal of "110" and the cube-root calculation result of "$\sqrt[3]{216} = 6$". In order to implement the cube-root calculation decimal integer "7" (the binary input number of "101,010,111"), multiple inputs C1 (1*), C2 (1*), C3 (2*), C5, C7 (3*) and C9 (3*) are introduced into the platform and hybridize with F1, F2 or F3 to form double strands of C1/F1, C2/F1, C3/F2, C7/F3 and C9/F3, isolating F1, F2 and F3 from DNA/GO platform. In this case, the three fluorescence outputs of ROX, HEX and Cy5 are lit up (Fig. 6, curve a7, b7 and c7) and defined as "1" in truth table, corresponding to the signal reporter "111" and exhibiting the 9-bit cube-root calculation result of "$\sqrt[3]{343} = 7$"

As shown in Fig. S7, the normalized fluorescence intensities (ROX, HEX and Cy5) at maximum peaks are plotted to make the cube-root calculations achieve ideal digital ON and OFF levels. To further verify the DNA hybridization between the inputs and the DNA/GO platform, the PAGE experiments are implemented, with the detail shown in Fig. S8. Also, based on the reacting mechanism, some advanced functions can be implemented, such as

more complex mathematic calculations, multipath detectors, and so on.

4. Conclusions

In conclusion, two mathematic calculations are established to realize the 6-bit square-root and 9-bit cube-root operation based on the same DNA/GO platform and the DNA hybridization mechanism. Firstly, the platform is prepared by fluorophore modified DNAs and GO. Individual DNA strands (F1-ROX, F2-HEX and F3-Cy5) modified by fluorophore have the abilities of adsorbing on the surface of GO and emitting low signals due to FRET, which forms the initial low-background platform. In order to implement the mathematic logic calculations, multiple inputs (6-bit inputs for square-root and 9-bit inputs for cube-root) are programmed to add into the DNA/GO platform and react with platform, emitting the corresponding fluorescence outputs and realizing corresponding calculation results. To our best knowledge, this is the first time that 6-bit square-root and 9-bit cube-root operations are constructed based on DNA hybridization mechanism and the same DNA/GO platform. Significantly, the realizations of the square-root operation and the cube-root operation are based on DNA hybridization programming and the affinity between GO and single/double DNA strands, which provide an easy approach and a powerful database to open up an inspiring horizon to DNA technology for designing programmability of innovative functional devices and concrete mathematic calculations. We promise to solve the problems of designing complexity and manufacturing cost of integrated devices in traditional computing by DNA-based biocomputing in the future.

Declaration of Competing Interest

The authors declare that they have no known competing financial interests or personal relationships that could have appeared to influence the work reported in this paper.

Acknowledgements

This work was supported by National Natural Science Foundation of China (91750205), National Key R&D Program of China)2018YFB1107202 (and K. C. Wong Education Foundation)GJTD-2018–08(.

Supplementary materials

Supplementary material associated with this article can be found, in the online version, at doi:10.1016/j.actbio.2020.09.054.

References

[1] I. Amlani, A.O. Orlov, G. Toth, G.H. Bernstein, C.S. Lent, G.L. Snider, Digital logic gate using quantum-dot cellular automata, Science 284 (5412) (1999) 289–291.
[2] Y. Huang, X. Duan, Y. Cui, L.J. Lauhon, K.-.H. Kim, C.M. Lieber, Logic gates and computation from assembled nanowire building blocks, Science 294 (5545) (2001) 1313–1317.
[3] A.P. De Silva, S. Uchiyama, Molecular logic and computing, Nat. Nanotechnol. 2 (7) (2007) 399–410.
[4] D. Fan, E. Wang, S. Dong, An intelligent universal system yields double results with half the effort for engineering a DNA "Contrary Logic Pairs" library and various DNA combinatorial logic circuits, Mater. Horiz. 4 (5) (2017) 924–931.
[5] P.A. de Silva, N.H.Q. Gunaratne, C.P. McCoy, A molecular photoionic AND gate based on fluorescent signalling, Nature 364 (6432) (1993) 42–44.
[6] L. Adleman, Molecular computation of solutions to combinatorial problems, Science 266 (5187) (1994) 1021–1024.
[7] G. Seelig, D. Soloveichik, D.Y. Zhang, E. Winfree, Enzyme-free nucleic acid logic circuits, Science 314 (5805) (2006) 1585–1588.
[8] M. You, G. Zhu, T. Chen, M.J. Donovan, W Tan, Programmable and multiparameter DNA-based logic platform for cancer recognition and targeted therapy, J. Am. Chem. Soc. 137 (2) (2015) 667–674.
[9] L. Feng, Z. Lyu, A. Offenhausser, D. Mayer, Multi-level logic gate operation based on amplified aptasensor performance, Angew. Chem. Int. Ed. 54 (26) (2015) 7693–7697.
[10] J. Chen, S. Zhou, J. Wen, Concatenated logic circuits based on a three-way DNA junction: a keypad-lock security system with visible readout and an automatic reset function, Angew. Chem. Int. Ed. 54 (2) (2015) 446–450.
[11] X.J. Jiang, D.K. Ng, Sequential logic operations with a molecular keypad lock with four inputs and dual fluorescence outputs, Angew. Chem. Int. Ed. 53 (39) (2014) 10481–10484.
[12] S. Mailloux, Y.V. Gerasimova, N. Guz, D.M. Kolpashchikov, E. Katz, Bridging the two worlds: a universal interface between enzymatic and DNA computing systems, Angew. Chem. Int. Ed. 54 (22) (2015) 6562–6566.
[13] D. Soloveichik, M. Cook, E. Winfree, J. Bruck, Computation with finite stochastic chemical reaction networks, Nat. Comput. 7 (2008) 615–633.
[14] G. Oster, A. Perelson, Chemical reaction networks, IEEE Trans. Circuits Syst. 21 (6) (1974) 709–721.
[15] A. Arkin, J. Ross, Computational functions in biochemical reaction networks, Biophys. J. 67 (2) (1994) 560–578.
[16] A. Hjelmfelt, E.D. Weinberger, J. Ross, Chemical implementation of neural networks and Turing machines, Proc. Natl. Acad. Sci. U. S. A. 88 (24) (1991) 10983–10987.
[17] G. Shinar, M. Feinberg, Structural sources of robustness in biochemical reaction networks, Science 327 (5971) (2010) 1389–1391.
[18] Y. Benenson, B. Gil, U. Ben-Dor, R. Adar, E. Shapiro, An autonomous molecular computer for logical control of gene expression, Nature 429 (6990) (2004) 423–429.
[19] E. Shapiro, B. Gil, Logic goes in vitro, Nat. Nanotechnol. 2 (2) (2007) 84–85.
[20] G. De Ruiter, M.E. Van Der Boom, Surface-confined assemblies and polymers for molecular logic, Acc. Chem. Res. 44 (8) (2011) 563–573.
[21] J. Andre ásson, U. Pischel, Smart molecules at work—Mimicking advanced logic operations, Chem. Soc. Rev. 39 (1) (2010) 174–188.
[22] M. Stojanovic, D. Stefanovic, S. Rudchenko, Exercises in molecular computing, Acc. Chem. Res. 47 (6) (2014) 1845–1852.
[23] F. Pu, J. Ren, X. Qu, Nucleic acids and smart materials: advanced building blocks for logic systems, Adv. Mater. 26 (33) (2014) 5742–5757.
[24] H. Li, W. Hong, S. Dong, Y. Liu, E. Wang, A resettable and reprogrammable DNA-based security system to identify multiple users with hierarchy, ACS Nano 8 (3) (2014) 2796–2803.
[25] L. Adleman, Molecular computation of solutions to combinatorial problems, Science 266 (5187) (1994) 1021–1024.
[26] L. Qian, E. Winfree, Scaling up digital circuit computation with DNA strand displacement cascades, Science 332 (6034) (2011) 1196–1201.
[27] N.C.J. Seeman, Nucleic-acid junctions and lattices, J. Theor. Biol. 99 (2) (1982) 237–247.
[28] Y. Tang, B. Ge, D. Sen, H. Yu, Functional DNA switches: rational design and electrochemical signaling, Chem. Soc. Rev. 43 (2) (2014) 518–529.
[29] S. Tyagi, F.R. Kramer, Molecular beacons: probes that fluoresce upon hybridization, Nat. Biotech. 14 (3) (1996) 303–308.
[30] J. Yang, R. Wu, Y. Li, Z. Wang, L. Pan, Q. Zhang, Z. Lu, C. Zhang, Entropy-driven DNA logic circuits regulated by DNAzyme, Nucleic. Acids. Res. 46 (16) (2018) 8532–8541.
[31] N.C. Seeman, Nanomaterials based on DNA, Annu. Rev. Biochem. 79 (2010) 65–87.
[32] T. Li, E. Wang, S. Dong, Potassium-lead-switched G-quadruplexes: a new class of DNA logic gates, J. Am. Chem. Soc. 131 (42) (2009) 15082–15083.
[33] L. Ma, A.P. Diao, Design of enzyme-interfaced DNA logic operations (AND, OR and INHIBIT) with an assaying application for single-base mismatch, Chem. Commun. 51 (50) (2015) 10233–10235.
[34] S. Bi, B. Ji, Z. Zhang, J. Zhu, Metal ions triggered ligase activity for rolling circle amplification and its application in molecular logic gate operations, Chem. Sci. 4 (4) (2013) 1858–1863.
[35] G. Seelig, D. Soloveichik, D.Y. Zhang, E. Winfree, Enzyme-free nucleic acid logic circuits, Science 314 (5805) (2006) 1585–1588.
[36] R. Peng, X. Zheng, Y. Lyu, L. Xu, X. Zhang, G. Ke, Q. Liu, C. You, S. Huan, W. Tan, Engineering a 3D DNA-logic gate nanomachine for bispecific recognition and computing on target cell surfaces, J, Am. Chem. Soc. 140 (31) (2018) 9793–9796.
[37] C. Zhou, D. Liu, C. Wu, S. Dong, E. Wang, Multifunctional graphene/DNA-based platform for the construction of enzyme-free ternary logic gates, ACS Appl. Mater. Inter. 8 (44) (2016) 30287–30293.
[38] C. Zhou, K. Wang, D. Fan, C. Wu, D. Liu, Y. Liu, E. Wang, An enzyme-free and DNA-based Feynman gate for logically reversible operation, Chem. Commun. 51 (51) (2015) 10284–10286.
[39] C. Zhou, C. Wu, Y. Liu, E. Wang, Effective construction of a AuNPs–DNA system for the implementation of various advanced logic gates, RSC Adv. 6 (108) (2016) 106641–106647.
[40] C. Zhou, D. Liu, C. Wu, Y. Liu, E. Wang, Integration of DNA and graphene oxide for the construction of various advanced logic circuits, Nanoscale 8 (40) (2016) 17524–17531.
[41] J. Li, A.A. Green, H. Yan, C. Fan, Engineering nucleic acid structures for programmable molecular circuitry and intracellular biocomputation, Nat. Chem. 9 (11) (2017) 1056–1067.
[42] Y.H. Lin, Y. Tao, F. Pu, J.S. Ren, X.G. Qu, Combination of graphene oxide and thiol-activated DNA metallization for sensitive fluorescence turn-on detection

of cysteine and their use for logic gate operations, Adv. Funct. Mater. 21 (23) (2011) 4565–4572.
[43] X.Q. Liu, R. Aizen, R. Freeman, O. Yehezkeli, I. Willner, Multiplexed aptasensors and amplified DNA sensors using functionalized graphene oxide: application for logic gate operations, ACS Nano 6 (4) (2012) 3553–3563.
[44] Y. He, Y.T. Chen, C.Y. Li, H. Cui, Molecular encoder–decoder based on an assembly of graphene oxide with dye-labelled DNA, Chem. Commun. 50 (59) (2014) 7994–7997.
[45] Y. Tao, Y. Lin, Z. Huang, J. Ren, X. Qu, Incorporating graphene oxide and gold nanoclusters: a synergistic catalyst with surprisingly high peroxidase-like activity over a broad pH range and its application for cancer cell detection, Adv. Mater. 25 (18) (2013) 2594–2599.
[46] M. Zhang, B.C. Ye, A reversible fluorescent DNA logic gate based on graphene oxide and its application for iodide sensing, Chem. Commun. 48 (30) (2012) 3647–3649.
[47] Y.H. Lin, Y. Tao, F. Pu, J.S. Ren, X.G. Qu, Combination of graphene oxide and thiol-activated DNA metallization for sensitive fluorescence turn-on detection of cysteine and their use for logic gate operations, Adv. Funct. Mater. 21 (23) (2011) 4565–4572.
[48] L. Wang, J. Zhu, L. Han, L. Jin, C. Zhu, E. Wang, S. Dong, Graphene-section, ACS Nano 6 (8) (2012) 6659–6666.
[49] Y. Xu, Q. Wu, Y. Sun, H. Bai, G. Shi, Three-dimensional self-assembly of graphene oxide and DNA into multifunctional hydrogels, ACS Nano 4 (12) (2010) 7358–7362.
[50] F. Li, J. Chao, Z.H. Li, S. Xing, S. Su, X.X. Li, S.P. Song, X.L. Zuo, C.H. Fan, B. Liu, W. Huang, L.H. Wang, L.H. Wang, Graphene oxide-assisted nucleic acids assays using conjugated polyelectrolytes-based fluorescent signal transduction, Anal. Chem. 87 (7) (2015) 3877–3883.
[51] F. Li, X. Liu, B. Zhao, J. Yan, Q. Li, A. Aldalbahi, J. Shi, S. Song, C. Fan, L. Wang, Graphene nanoprobes for real-time monitoring of isothermal nucleic acid amplification, ACS Appl. Mater. Inter. 9 (18) (2017) 15245–15253.
[52] C.Y. Zhou, H.M. Geng, P.F. Wang, C.L. Guo, Programmable DNA nanoindicator-based platform for large-scale square root logic biocomputing, Small 15 (49) (2019) 1903489.
[53] H.M. Geng, C.Y. Zhou, C.Y. Guo, DNA-based digital comparator systems constructed by multifunctional nanoswitches, Nanoscale 11 (45) (2019) 21856–21866.
[54] W.S. Hummers, R.E. Offeman, Preparation of graphitic oxide, J. Am. Chem. Soc. 80 (1958) 1339.
[55] C.Y. Zhou, H.M. Geng, C.L. Guo, Design of DNA-based innovative computing system of digital comparison, Acta Biomater 80 (2018) 58–65.